Quantitative analysis of the ubiquitin-proteasome system under proteolytic and folding stressors

Jeremy J. Work[1] and Onn Brandman[1]*

[1]Department of Biochemistry, Stanford University, Stanford CA USA
*For correspondence:onn@stanford.edu

Abstract Aging, disease, and environmental stressors are associated with failures in the ubiquitin-proteasome system (UPS), yet a quantitative understanding of how stressors affect the proteome and how the UPS responds is lacking. Here we assessed UPS performance and adaptability in yeast under stressors using quantitative measurements of misfolded substrate stability and stress-dependent UPS regulation by the transcription factor Rpn4. We found that impairing degradation rates (proteolytic stress) and generating misfolded proteins (folding stress) elicited distinct effects on the proteome and on UPS adaptation. Folding stressors stabilized proteins via aggregation rather than overburdening the proteasome, as occurred under proteolytic stress. Still, the UPS productively adapted to both stressors using separate mechanisms: proteolytic stressors caused Rpn4 stabilization while folding stressors increased *RPN4* transcription. In some cases, adaptation completely prevented loss of UPS substrate degradation. Our work reveals the distinct effects of proteotoxic stressors and the versatility of cells in adapting the UPS.

Introduction

The ubiquitin-proteasome system (UPS) is the primary route for the disposal of defective proteins in eukaryotic cells (Hershko et al. 1983, 1984; Lecker, Goldberg, and Mitch 2006). Aging, genetic mutations, and environmental changes all challenge the UPS and can lead to accumulation of defective proteins ("proteotoxic stress"), which is a hallmark of many neurodegenerative diseases, including Alzheimer's disease, Parkinson's disease, Huntington's disease, and amyotrophic lateral sclerosis (Labbadia and Morimoto 2015; Sweeney et al. 2017; Klaips, Jayaraj, and Hartl 2018). Characterizing the performance and adaptability of the UPS in clearing defective proteins under proteotoxic stressors is thus likely to aid in understanding numerous diseases.

In the UPS, ubiquitin ligases modify selected proteins with polyubiquitin chains that target them for degradation by the 26S proteasome, a 2.5 MDa protein complex composed of 33 unique subunits (Voges, Zwickl, and Baumeister 1999). To simultaneously and stoichiometrically drive the expression of dozens of proteasomal components along with other UPS-related genes, eukaryotes have evolved master transcriptional regulators that target all proteasome genes, as well as ubiquitin, ubiquitin ligases, and extrinsic proteasome factors (Mannhaupt et al. 1999; Lundgren et al. 2003; Meiners et al. 2003; Kraft et al. 2006; Xu et al. 2008; Sato et al. 2009; Radhakrishnan et al. 2010). In budding yeast, this master regulation occurs via the transcription factor Rpn4 (Xie and Varshavsky 2001).

To adapt the expression of UPS components based on cellular needs, cells regulate Rpn4 levels via multiple stress-sensitive mechanisms. These include proteasomal degradation of Rpn4 via two encoded degradation signals (degrons) that target it to the proteasome: one ubiquitin-independent signal at the N-terminus, and one signal recognized by the E3 ubiquitin ligase Ubr2 (Ha, Ju, and Xie 2012; L. Wang et al. 2004). Due to these degrons, Rpn4 has a short half-life of 2 minutes and will therefore quickly accumulate if the proteasome is impaired (Xie and Varshavsky 2001). Additionally, *RPN4* is transcriptionally regulated by several stress-sensitive transcription factors, including Yap1, a responder to oxidative stress; Pdr1/3, the drivers of the pleiotropic drug resistance response; and Hsf1, the driver of the heat shock response (HSR)(Hahn, Neef, and Thiele 2006; Ma and Liu 2010; Temple, Perrone, and Dawes 2005; Moye-Rowley 2003). We term the collective, stress-responsive transcriptional regulation of the UPS through Rpn4 the proteasome stress response ("PSR"), analogous to terminology used to describe other transcriptional stress responses like the HSR.

While the PSR has been demonstrated to respond to proteotoxic stressors (Xie and Varshavsky 2001; X. Wang et al. 2010; Schmidt et al. 2019), quantification of its effectiveness at combating such stressors and the relative contributions of its distinct activation mechanisms have not been investigated in diverse proteotoxic conditions. Two ways stressors may increase levels of misfolded proteins are to 1) cause proteins to misfold or obstruct their folding ("folding stress"), or 2) impair degradation rates of misfolded proteins ("proteolytic stress") (Figure 1A). A naive expectation is that folding and proteolytic stressors have overlapping effects on the proteome and UPS. For example, misfolded proteins generated by a folding stressor may become targeted to the proteasome, increasing competition between proteasome substrates and thereby lowering degradation rates for each substrate (i.e. a folding stressor leading indirectly to proteolytic stress). Conversely, UPS substrates that are stabilized by a proteolytic stressor may potentiate the misfolding of other proteins (i.e. a proteolytic stressor indirectly leading to folding stress), as has been observed when expression of one misfolded protein causes others to misfold (Satyal et al. 2000; Gidalevitz et al. 2006, 2009). However, these hypotheses have not yet been quantitatively evaluated. Furthermore, it is unknown if activation of the PSR fully neutralizes proteotoxic challenges ("perfect adaptation"), if cells accumulate defective proteins in spite of PSR activation ("partial adaptation"), if cells overreact to these challenges ("overadaptation"), and whether cellular responses are distinct for proteolytic and folding stressors.

We systematically characterized the performance and adaptability of the UPS under diverse stress conditions in yeast using quantitative measurements of UPS performance (measured by the stability of misfolded reporter substrates) and PSR-mediated adaptation (transcriptional activation of Rpn4 target genes as measured by a synthetic reporter). We unexpectedly found that proteolytic and protein folding stressors stabilized misfolded proteins and activated the PSR through separate, non-overlapping mechanisms. Proteasomal inhibition (a proteolytic stressor) blocked degradation of misfolded proteins and stabilized Rpn4 without increasing *RPN4* transcription. By contrast, the addition of the amino acid analogs canavanine and AZC (folding stressors) caused aggregation of misfolded proteins rather than their targeting to the proteasome, yet still activated the PSR by driving transcriptional activation of *RPN4* without increasing Rpn4 stability. The PSR productively responded to both proteolytic and protein folding stressors despite their different underlying mechanisms for increasing misfolded

88 protein levels. In both cases, this included perfect or near-perfect adaptation. Our work reveals
89 the adaptability of the UPS and provides a framework to quantitatively understand how cells
90 regulate the UPS in response to proteotoxicity and disease-causing states.
91

92 Results

93

94 Clearance of defective proteins scales with the PSR

95 To investigate the UPS under stress conditions, we built quantitative reporters that measure the
96 performance of the UPS and the activity of the cell's primary transcriptional effector of the UPS,
97 the PSR. Because a major role of the UPS is to identify and degrade defective proteins, we
98 defined "UPS performance" as the ability to degrade reporter proteins containing constitutively
99 misfolded domains. We designed two UPS substrates, Cyto-Deg and ERm-Deg, consisting of a
100 green fluorescent protein (sfGFP) fused to a degron sequence featuring a cluster of
101 hydrophobic residues (Maurer et al. 2016)(Figure 1B). Cyto-Deg localizes to the cytosol and is
102 dependent on Hsp70 for degradation (Maurer et al. 2016). ERm-Deg localizes to the
103 endoplasmic reticulum (ER) membrane—likely because its C-terminal degron is also an ER
104 targeting signal—and is ubiquitylated by the ER-membrane-localized ubiquitin ligase Doa10
105 (Maurer et al. 2016). Doa10 is part of the ERAD-C pathway, which targets ER transmembrane
106 proteins with a misfolded domain in the cytosol (Ruggiano, Foresti, and Carvalho 2014). Thus,
107 expression of both Cyto-Deg and ERm-Deg leads to misfolded protein domains in the cytosol,
108 but they are efficiently degraded by the proteasome via separate pathways. Evaluating the
109 stability of both degrons therefore informs on the state of the proteasome, the shared feature in
110 their degradation. To control for protein synthesis rate, we expressed a red fluorescent protein
111 (mCherry) upstream of the sfGFP-degron fusion, separated by two tandem T2A peptide-
112 skipping sequences (Donnelly et al. 2001; Szymczak and Vignali 2005). mCherry and the
113 sfGFP-degron are synthesized stoichiometrically, but mCherry is detached during translation
114 and escapes UPS targeting. The sfGFP/mCherry ratio is therefore proportional to the stability of
115 the degron-fused protein, where a high ratio indicates high stability and a low ratio indicates low
116 stability. Cyto-Deg and ERm-Deg were both capable of reporting on UPS performance, as
117 evidenced by an increase in the sfGFP/mCherry ratio upon treatment with a 40 μM dose of the
118 proteasome inhibiting drug bortezomib (Figure 1C).
119 To measure the PSR, we built a synthetic promoter specifically sensitive to changes in
120 the PSR. The PSR is driven by the binding of Rpn4 to a DNA motif called the proteasome-
121 associated control element (PACE), which is found in the promoters of all proteasomal subunits
122 and many proteasome-associated factors (Mannhaupt et al. 1999; Shirozu, Yashiroda, and
123 Murata 2015). The PSR reporter features four tandem copies of the PACE sequence along with
124 a minimal promoter to drive expression of sfGFP (Figure 1D). We validated the reporter's
125 sensitivity by blocking Rpn4 degradation with bortezomib and observing a monotonic increase in
126 GFP expression in response (Figure 1D). This increase corresponded to increased levels of
127 hemagglutinin-tagged endogenous Rpn4 (Figure 1D).
128 We first used our reporters to evaluate how modulating the PSR affects UPS
129 performance in unstressed conditions by genetically altering the constitutive levels of Rpn4. To
130 reduce Rpn4 levels, we replaced the endogenous *RPN4* promoter with a weaker promoter
131 (*pCYC1*). To increase Rpn4 levels, we deleted factors necessary for Rpn4 degradation (Ubr2 or

132 Mub1)(Ju et al. 2008; L. Wang et al. 2004), or expressed a second copy of *RPN4* from a single-
133 copy plasmid. PSR activity was inversely correlated with Cyto-Deg and ERm-Deg stability,
134 demonstrating that PSR activity is tightly coupled to UPS performance (Figure 1E).
135

136 Proteotoxic stressors elicit multiple adaptive regimes

137 To understand the adaptive potential of the UPS, we investigated the role of the PSR in clearing
138 defective proteins during proteotoxic stress. We achieved this by measuring the PSR and
139 degron stability in cells after 5 hour treatment with three proteotoxic compounds: bortezomib,
140 canavanine (an arginine analog), and azetidine-2-carboxylic acid ("AZC"; a proline analog).
141 Bortezomib directly inhibits the proteasome to cause proteolytic stress. Canavanine and AZC
142 directly disrupt protein folding when incorporated into newly synthesized proteins, causing
143 folding stress. By measuring cellular responses after 5 hours, we aimed to capture the system
144 after adaptive mechanisms had taken effect. At the highest concentrations tested, all three
145 stressors increased the stability of both Cyto-Deg and ERm-Deg and induced the PSR,
146 consistent with their proteotoxicity (Figure 2A). We were concerned that high doses of
147 canavanine and AZC would directly disrupt PSR reporter inducibility, so we limited the
148 concentrations of canavanine and AZC to a range in which the PSR reporter remained
149 comparably inducible by 5 μM bortezomib and could therefore reliably report on PSR activity
150 (Figure 2B).
151 To determine how the UPS adapts to each stressor, we compared the relationship
152 between UPS performance and PSR activation (Figure 2C). *Perfect adaptation*, a regime where
153 cells respond to a stressor without any loss of UPS performance, would be observed as
154 activation of the PSR without any change in UPS performance. *Non-adaptation* would manifest
155 as a lack of PSR activation with concurrent loss of UPS performance. *Partial adaptation* would
156 present as an intermediate between these two regimes, where the PSR activates but UPS
157 performance still declines. Finally, *overadaptation* would be evidenced by PSR activation
158 coupled to an increase in UPS performance. Strikingly, cells exhibited near-perfect adaptation in
159 response to low doses of bortezomib (≤2.5 μM), as the PSR was activated but stability
160 remained the same or nominally increased for both degrons (Figure 2A,2D). At higher doses
161 (>2.5 μM), the response to bortezomib resulted in partial adaptation, showing decreasing UPS
162 performance as bortezomib dose increased despite PSR activation. Responses to canavanine
163 and AZC caused a divergent response: UPS adaptation was perfect or overadaptive up to 200
164 μM and 1 mM respectively for Cyto-Deg but partial for ERm-Deg. These observations suggest
165 UPS adaptation is highly effective but becomes less so under severe stressors, as noted by an
166 increase in stability of both degrons at high doses of bortezomib and ERm-Deg at several doses
167 of canavanine and AZC. Furthermore, the divergence of adaptive response between proteolytic
168 stressors (partial adaptation regardless of degron monitored) and folding stressors (degron-
169 specific adaptation regimes) suggests that these stressors cause distinct effects on cells.
170

171 Activating the PSR improves UPS performance under stress

172 To understand the limitations of the PSR, we next investigated why adaptation was imperfect for
173 ERm-Deg under AZC and canavanine treatment and for both degrons at high doses of
174 bortezomib. One model to explain these results is that the PSR is insufficiently activated in

these conditions, resulting in a PSR that cannot fully compensate for the increased proteotoxic burden. Alternatively, the stressors we applied may exceed the capacity of the PSR to increase UPS performance. To distinguish between these models, we tested whether enhancing the PSR by expressing a second copy of *RPN4* improves degradation in stress conditions. Indeed, it was recently shown that *RPN4* overexpression improves UPS performance in clearing mislocalized ER proteins or defective ribosome proteins in the cytosol (Schmidt et al. 2019; Tye et al. 2019). As expected, expressing a second copy of *RPN4* in the absence of stress increased the PSR and destabilized Cyto-Deg and ERm-Deg relative to an empty vector control (Figure 1E and 3). Under stress conditions, the addition of a second *RPN4* copy lowered degron stability for nearly all concentrations of bortezomib, canavanine, or AZC tested (Figure 3). We conclude that activating the PSR is sufficient to improve UPS performance under all stressors and that Rpn4 is insufficiently activated to clear specific substrates in partially adaptive regimes.

Folding stressors activate the PSR predominantly via transcription of *RPN4*

Because amino acid analogs caused a degron-specific adaptive regime while bortezomib did not (Figure 2D), we reasoned that these stressors may be sensed differently by cells. Proteasome inhibition via bortezomib is likely to activate the PSR by impaired degradation of Rpn4, although it may also cause transcriptional activation of *RPN4*. In contrast, it is unclear whether the folding stressors canavanine and AZC activate the PSR through creation of new proteasome substrates that compete with Rpn4 for degradation and stabilize it (i.e. an indirect proteolytic stress), transcriptional activation of *RPN4*, or both. Indeed, canavanine and AZC robustly activate Hsf1, a transcriptional activator of *RPN4* (Hahn, Neef, and Thiele 2006; Yamamoto et al. 2008; Alford and Brandman 2018). We therefore investigated the role of transcriptional regulation of *RPN4* in activating the PSR during stressor treatment. Consistent with previous work, a reporter of Hsf1 activity (Brandman et al., 2012) robustly activated in the presence of canavanine and AZC (up to 6- and 7-fold activation at their highest concentrations, respectively), with comparatively weak (up to 2-fold) maximal activation by bortezomib (Figure 4A). Because Hsf1 targets the *RPN4* promoter (Hahn, Neef, and Thiele 2006), we predicted that the promoter of RPN4 (*pRPN4)* should be upregulated in canavanine and AZC stress. We measured the activity of *pRPN4* using a *pRPN4:GFP* plasmid reporter and found that bortezomib did not activate *pRPN4*, while canavanine and AZC modestly increased the promoter's activity (1.6- and 1.3-fold)(Figure 4B). This is consistent with a model that folding stressors but not proteolytic stressors upregulate the PSR via transcriptional regulation of *RPN4*.

Folding stressors do not increase UPS substrate load

Given the similarity in magnitude of PSR activation and *pRPN4* induction in canavanine and AZC (Figure 2A and 4B), we hypothesized that PSR activation by these two stressors is fully accounted for by transcriptional targeting of *pRPN4*, with little or no contribution through stabilization of Rpn4. By contrast, bortezomib does not activate *pRPN4* (Figure 4B), and presumably induces the PSR through stabilization of Rpn4 alone. To determine the contribution of Rpn4 stabilization to the PSR under canavanine and AZC treatments, we disabled transcriptional regulation by engineering strains in which the genomic copy of *RPN4* is under the control of the *YEF3* promoter (*pYEF3*), which is not targeted by Hsf1 but retains the same

219 approximate basal expression (1.23 fold basal, s.e.=.027). In the absence of stress-sensitive
220 transcriptional regulation of *RPN4*, PSR induction was retained in bortezomib treatment, but
221 partially lost in canavanine and fully lost in AZC treatment (Figure 4C). We therefore predicted
222 that loss of promoter-mediated PSR activation will impair adaptation to folding stressors and
223 minimally affect proteolytic stressors. Indeed, Cyto-Deg and ERm-Deg stability was sensitized
224 to canavanine and AZC in the *pYEF3:RPN4* background, evidenced by greater degron
225 stabilization relative to wildtype (Figure 4D). Furthermore, degron stabilization was greater
226 under AZC treatment than canavanine treatment, which correspondingly had a greater loss of
227 PSR activation in the *pYEF3:RPN4* background. We conclude that protein folding stress caused
228 by canavanine and AZC does not lead to stabilization of Rpn4, and instead UPS adaptation
229 under these stressors occurs predominantly via increased *RPN4* transcription.
230 Transcriptional activation of the PSR by canavanine and AZC (Figure 4C) could be
231 specific to these treatments or it could be the general response to folding stressors. To test the
232 generality of this phenomenon, we increased the likelihood of protein misfolding by raising the
233 steady state temperature of wildtype yeast from 30°C to 37°C. This was sufficient to activate the
234 HSR, but caused no change in PSR activation (Figure 4E). Consistent with a model in which
235 folding stress does not increase the burden of substrates on the proteasome, deletion of protein
236 chaperone genes (*HSC82*, *SSA2*, *HSP104*) increased the HSR but not the PSR (Figure 4F).
237 These results suggest that proteins that misfold due to folding stressors do not create proteolytic
238 stress.
239

240 Folding stressors cause aggregation and result in failure to target 241 aggregation-prone substrates to the proteasome

242 Given that the misfolded proteins generated by folding stressors did not appear to increase
243 proteasome burden, we explored the possibility that the misfolded proteins are instead
244 sequestered into aggregates in which they are protected from proteasomal degradation. Indeed,
245 it has been previously reported that AZC can cause aggregation of endogenous proteins (Weids
246 and Grant 2014), and that aggregation can be a mechanism for avoiding degradation (Wallace
247 et al. 2015). Because canavanine and AZC robustly activate the HSR, a response that is driven
248 by a drop in protein chaperone availability (Zheng et al. 2016; Alford and Brandman 2018), we
249 reasoned that chaperones become limiting under folding stressors and this may drive protein
250 aggregation. To test this, we boosted Hsf1 activity to increase chaperone levels and determined
251 if this would increase the stability of our degron reporters during canavanine and AZC treatment.
252 We expressed an extra copy of Hsf1 with an N-terminal truncation that renders it constitutively
253 active ($Hsf1_{\Delta 1\text{-}147}$) (Sorger 1990) in a strain expressing *RPN4* from the *CYC1* promoter (to
254 eliminate the confounding effect that Hsf1 activates *pRPN4*). $Hsf1_{\Delta 1\text{-}147}$ reduced Cyto-Deg and
255 ERm-Deg levels in response to canavanine and AZC but not bortezomib (Figure 5A). These
256 results suggest that the decrease in UPS performance due to canavanine and AZC is resolvable
257 by increasing chaperone levels, supporting that they cause protein folding stress, while
258 bortezomib does not. This chaperone dependence for degradation is consistent with the
259 hypothesis that folding stressors result in sequestration of UPS substrates into aggregates.
260 To directly assess the presence of aggregates in canavanine and AZC treated cells, we
261 performed fluorescence microscopy on cells expressing Cyto-Deg or ERm-Deg. Canavanine
262 and AZC caused GFP in both Cyto-Deg and ERm-Deg to form inclusions (Figure 5B).

263 Consistent with previous reports (Weids and Grant 2014), 4 mM AZC also increased expression
264 of Hsp104 and relocalized it into foci (Figure 5C) in cells without a degron reporter. A similar
265 response was observed with 800 μM canavanine. This change in Hsp104 localization suggests
266 that endogenous proteins (not just our synthetic reporters) are sequestered into aggregates in
267 the presence of canavanine and AZC. By contrast, even a high dose (40 μM) of bortezomib that
268 strongly increased degron levels did not alter the localization of the degrons or induce Hsp104
269 expression. These observations suggest that canavanine and AZC cause protein folding stress
270 that drives misfolded proteins into aggregates rather than targeting them to the proteasome.
271 Under this model, folding stress fails to stabilize Rpn4 because it does not produce proteasome
272 substrates that compete with Rpn4 for degradation.
273 If aggregation interferes with the degradation of misfolded proteins by the UPS, we
274 predicted that highly soluble proteasome substrates that escape aggregation during folding
275 stress would continue to be degraded normally. To test this prediction, we built a third degron
276 reporter, ATA-Deg (a "CAT tail" degron), which was demonstrated in previous work to be poly-
277 ubiquitylated and targeted for proteasomal degradation, but whose six-peptide degron sequence
278 ("ATAATA") is soluble (Sitron and Brandman, 2019). Accordingly, ATA-Deg was diffuse
279 throughout the cytosol even under high doses of canavanine, AZC, or bortezomib (Figure 6A).
280 Bortezomib treatment increased the stability of ATA-Deg, indicating sensitivity to proteolytic
281 stress. Conversely, ATA-Deg levels were constant or decreased under all concentrations of
282 canavanine and AZC treatment (Figure 6B), suggesting that folding stress does not impair
283 degradation of ATA-Deg. Consistent with this and in contrast to Cyto-Deg and ERm-Deg (Figure
284 5A), ATA-Deg stability was not affected by expression of $Hsf1_{\Delta 1\text{-}147}$ under folding stressors. We
285 conclude that folding stressors sequester aggregation-prone UPS substrates without disrupting
286 degradation of soluble substrates (Figure 6D).
287

288 ## Discussion

289 Here we assessed the performance and adaptability of the UPS in yeast under stress conditions
290 using quantitative measurements of UPS performance and the adaptive transcriptional
291 response of the UPS (the "proteasome stress response," or PSR). We found that proteolytic and
292 protein folding stressors stabilized misfolded proteins through separate, non-overlapping
293 mechanisms, with the former blocking degradation of misfolded proteins and the latter resulting
294 in their aggregation rather than their targeting to the proteasome. Despite a difference in the
295 underlying proteostasis defect, the UPS productively responded to both proteolytic and folding
296 stressors, and in both cases, this included perfect or near-perfect adaptation (no loss in
297 degradation performance) for some substrates (Figure 2D).
298 The perfect and near-perfect adaptation we observed for the UPS implies the existence
299 of an underlying network that can mechanistically achieve this (Ferrell 2016). In the case of
300 folding stress, *RPN4* is activated transcriptionally (Figure 4B and 4C), likely by Hsf1, to achieve
301 perfect adaptation for proteins that aggregate in the cytosol. This intervention may cause
302 increased degradation rates of soluble proteasome substrates, an intriguing consequence of a
303 system that tunes the UPS to "problem" proteins that are poor UPS substrates (aggregated
304 proteins). This substrate-specific adaptation likely occurs to some degree in all stress responses
305 that use concerted transcriptional regulation to address substrates with distinct adaptive needs.

306 Under proteolytic stress, where Rpn4 is stabilized and its activation rescues the
307 degradation of other proteasomal substrates (Figure 2D), perfect adaptation requires that the
308 increase in Rpn4 activity compensate for the loss in degradation of proteasome substrates. This
309 may occur via a combination of the multiple degrons present on Rpn4 and could also involve
310 post-translational regulation of Rpn4, which is ubiquitylated and phosphorylated (Ju et al. 2007;
311 L. Wang et al. 2004). Additionally, proteasome inhibition may cause the buildup of substrates
312 that selectively outcompete Rpn4 but not other substrates, making Rpn4 levels hypersensitive
313 to proteolytic stress. Understanding the range of substrates and conditions for which perfect or
314 near-perfect adaptation occurs and its underlying mechanisms is an important topic for future
315 study.
316 Our data suggest that protein folding stressors do not burden the proteasome with
317 increased overall substrate load (Figure 4C, 4F, and 4G). Instead, misfolding causes the
318 sequestration of aggregation-prone substrates into inclusions and a resultant loss of their UPS
319 targeting. This cellular behavior that favors aggregation over degradation is contrary to what has
320 been observed for certain thermolabile proteins, which presumably misfold upon temperature
321 increase but are nevertheless degraded (Betting and Seufert 1996; Dohmen, Wu, and
322 Varshavsky 1994; Downey et al. 2006). Our work instead suggests that endogenous proteins in
323 yeast have evolved to aggregate rather than become targeted by the UPS during folding stress.
324 This conclusion is in line with experiments demonstrating that the yeast proteome forms
325 aggregates instead of being targeted to the UPS in response to acute heat shock (Wallace et al.
326 2015). Such a strategy has the advantage of preserving proteins that may be refolded at a later
327 time after stressors are removed, allowing a faster recovery with less energy expenditure. It may
328 also prevent adverse effects of high UPS activity, which has been shown to confer growth
329 defects (X. Wang et al. 2010). However, by promoting aggregation, cells create a risk for
330 proteotoxicity and entrance into a pathogenic state, as observed in the numerous
331 neurodegenerative diseases characterized by buildup of misfolded proteins in neurons
332 (Labbadia and Morimoto 2015; Sweeney et al. 2017). In yeast, even inert insoluble proteins can
333 cause growth defects (Geiler-Samerotte et al. 2011). Moving forward, it remains to be
334 determined whether human cells, particularly neurons, make a similar tradeoff that favors
335 aggregation over degradation and whether this tradeoff puts them at risk for disease.
336 Because there is no surge of proteasome substrates when cells are faced with folding
337 stressors, upregulation of the PSR in these conditions relies entirely upon the stress-sensitive
338 transcriptional upregulation of *RPN4* rather than stabilization of the Rpn4 protein. Cells may
339 have a divergent ability to sense different protein quality failures, as suggested by better
340 adaptation of Cyto-Deg vs. ER-Deg under folding stress. Despite the absence of a UPS "traffic
341 jam," upregulation of the PSR during these stressors still improves the cell's ability to degrade
342 aggregation-prone proteins (Cyto-Deg and ERm-Deg in AZC and canavanine treatment). This
343 could be because of enhanced PSR activity coinciding with the emergence of aggregates limits
344 their formation, or because misfolded proteins are in an equilibrium between aggregated and
345 soluble states and boosting the PSR adjusts this equilibrium point. Exploration of these
346 possibilities is an exciting prospect for preventing and reversing diseases characterized by
347 protein aggregation.
348
349

Materials and Methods

Yeast strain construction and culturing methods

All yeast strains were created from BY4741. Yeast cultures were grown at 30 °C (unless otherwise noted) in yeast extract peptone dextrose (YPD) media or synthetic dropout (SD) media.

Strain construction was done by transforming cells with a crude PCR product bearing 40 base pair overhangs homologous to the target genomic locus, a selection cassette for either antibiotic selection in YPD or auxotrophic selection in SD, and any other desired sequences. Deletion strains were constructed in the BY4741 background via transformation with antibiotic selection cassettes (NATMX6 or KANMX6), amplified with overhangs flanking the open reading frame to be deleted. The *pCYC1:RPN4* and *pYEF3:RPN4* strains were constructed via transformation by inserting a His3 cassette and 1000bp of either *pCYC1* or *pYEF3* immediately upstream of the *RPN4* open reading frame. The Hsp104-mKate2 strain was generated via transformation by inserting the yeast-optimized mKate2 coding sequence and a hygromycin selection cassette immediately downstream of the endogenous *HSP104* open reading frame. All transformants were verified by genomic PCR.

Plasmids used in this study were cloned using the Gibson Assembly method and the NEBuilder HiFi DNA Assembly Master Mix (New England Biolabs). The PSR reporter, HSR reporter, *pRPN4:GFP* reporter, Cyto-Deg, ER-Deg, and ATA-Deg plasmids were expressed from high-copy plasmids containing a Ura3 selection cassette. For *RPN4* overexpression experiments, a single-copy plasmid with a His5 selection cassette and either *pRPN4:RPN4* or no insert was co-expressed with the fluorescent reporters mentioned above. For experiments involving the expression of truncated *HSF1*, a single-copy plasmid with a Leu2 selection cassette and either $pHSF1{:}HSF1_{\Delta 1\text{-}147}$ or no insert was co-expressed with the fluorescent reporters mentioned above.

The degron sequence for Cyto-Deg is SIFYHIGTDLWTLSEHYYEGVLSLVASVIISGR, and the degron sequence for ERm-Deg is GVKHFVFFTMFSIMPAINFPLGR (Ruggiano, Foresti, and Carvalho 2014; Maurer et al. 2016). Both sequences were connected to sfGFP by a GSGS linker.

Fluorescent reporter assay measurements

All experiments were performed with at least three biological replicates measured on different days. For experiments testing the effects of drug stressors, stock solutions of the drugs were prepared in advance (5 mM bortezomib in ethanol, 0.5 M canavanine in water, 0.5 M AZC in water). Yeast were inoculated into selective SD media such that after overnight growth (>12 hours) in aerated culture tubes, their OD600 was between 0.05 and 0.3. Yeast were then diluted to 0.05 in a 96-well plate and incubated for 30 minutes. The drug stressors were serial diluted to 50x concentrations, then added to cells 1:50 to reach 1x concentrations. The yeast were grown for 5 hrs while shaking at 1050 rpm. Fluorescence was measured on a BD Accuri C6 flow cytometer (BD Biosciences).

Measurements of cells treated with multiple drugs (Figure 2C) differed in that drug stressors were added at two distinct timepoints according to the schematic in Figure 2c. Measurements of the knockout strains (Figure 4G) differed in that upon overnight growth, cells

394 with OD600 between 0.05 and 0.3 were immediately measured. Comparative measurements of
395 cells in 30 °C or 37 °C growth (Figure 4F) differed in that they were grown overnight to
396 saturation at 30 °C, diluted to log phase and grown for 5 hours at 30 °C, then split for growth at
397 30 °C or 37 °C at dilutions such that they were in log phase after overnight growth, then
398 immediately measured.
399

400 **Reporter quantification**

401 All quantitative analysis was performed using MATLAB v8.6 (MathWorks). For the PSR, HSR,
402 and *pRPN4:GFP* reporters, the GFP fluorescence measurements were normalized to forward
403 scatter for each cell. For ERm-Deg, Cyto-Deg, and ATA-Deg, GFP fluorescence measurements
404 were normalized to RFP. In experiments comparing genetic backgrounds or growth
405 temperatures (Figure 1E, 4F, and 4G), samples were normalized to a corresponding wildtype
406 control, which was set to 1. In titration experiments, samples were normalized to a
407 corresponding no-treatment control that was set to 1. For titrations in backgrounds being
408 compared to wildtype (the nonblack or broken lines in Figure 3a, 4cd, 5a), the no-treatment
409 control was set to its mean fold value relative to the no-treatment control in solid black.
410

411 **Imaging**

412 Cells expressing Cyto-Deg, ERm-Deg, ATA-Deg, or Hsp104-mKate2 were inoculated into
413 selective SD media such that after overnight growth (>12 hours) in aerated culture tubes, their
414 OD600 was between 0.1 and 0.4. Yeast were diluted to 0.1 and incubated for 30 minutes. Drug
415 stressors were then added and the cells were incubated for 5 hours. Cells were concentrated
416 through pelleting and resuspension, then immobilized on glass slides pre-treated with
417 concanavalin A.
418 Imaging was performed on an Eclipse 80i microscope (Nikon) with an X-Cite 120LED
419 light source (Excelitas Technologies) and using a 100x 1.40 NA oil immersion lens, controlled
420 via MetaMorph v7.10.2.240 software (Molecular Devices). Images were captured with an Andor
421 DR-328G-CO1-SIL Clara CCD monochrome camera (Andor Technology).
422

423 **Immunoblotting**

424 SDS-PAGE was performed on samples using Novex Nupage 4–12% Bis-Tris gels (Thermo
425 Fisher Scientific). Samples were then transferred onto 0.45-um nitrocellulose membranes (Bio-
426 Rad) using a standard wet transfer protocol. Membranes were blocked with 5% milk in Tris-
427 buffered saline with Tween for one hour at room temperature. They were then stained with
428 1:2,000 Pierce mouse anti-GFP (Thermo Fisher Scientific) primary antibody overnight at 4ºC,
429 followed by IRDye 800CW donkey anti-mouse (LiCor Biosciences) for three hours at room
430 temperature. Membranes were then scanned using a LiCor Odyssey (LiCor Biosciences).
431
432

433 **Acknowledgements**

434 We thank Dr. R.R. Kopito, Dr. J.E. Ferrell Jr., B.D. Alford, V. Ambati, L. Persson, C.S. Sitron,
435 and S.L. Ergun for their helpful comments during manuscript preparation. We additionally thank
436 Dr. J. Frydman, Dr. A. Matouschek, Dr. Y. Merbl, Dr. Z.H. Davis, and Dr. Z.A. Jaafar for helpful

discussion. We thank J. Giafaglione for construction of the *pHSF1:HSF1*$_{\Delta 1\text{-}147}$ expression plasmid and B.D. Alford for construction of the HSR reporter plasmid. We thank B.D. Alford, J. Park, and C.S. Sitron for assistance in strain building. We thank Dr. A.F. Straight and O.K. Smith for microscope usage and guidance. This work was supported by Stanford University (O.B.) and the National Institute of General Medical Sciences of the US National Institutes of Health (grant No. T32GM007276 to J.J.W.).

Competing interests

We declare no competing interests.

Author contributions

J.J.W. and O.B. designed the experiments and wrote the manuscript. J.J.W. performed the experiments and analysis.

References

Alford, Brian D., and Onn Brandman. 2018. “Quantification of Hsp90 Availability Reveals Differential Coupling to the Heat Shock Response.” *The Journal of Cell Biology* 217 (11): 3809–16.

Betting, J., and W. Seufert. 1996. “A Yeast Ubc9 Mutant Protein with Temperature-Sensitive in Vivo Function Is Subject to Conditional Proteolysis by a Ubiquitin- and Proteasome-Dependent Pathway.” *The Journal of Biological Chemistry* 271 (42): 25790–96.

Dohmen, R. J., P. Wu, and A. Varshavsky. 1994. “Heat-Inducible Degron: A Method for Constructing Temperature-Sensitive Mutants.” *Science* 263 (5151): 1273–76.

Donnelly, Michelle L. L., Martin D. Ryan, Amit Mehrotra, David Gani, Lorraine E. Hughes, Garry Luke, and Xuejun Li. 2001. “Analysis of the Aphthovirus 2A/2B Polyprotein ‘cleavage’ Mechanism Indicates Not a Proteolytic Reaction, but a Novel Translational Effect: A Putative Ribosomal ‘skip.’” *Journal of General Virology*. https://doi.org/10.1099/0022-1317-82-5-1013.

Downey, Michael, Rebecca Houlsworth, Laura Maringele, Adrienne Rollie, Marc Brehme, Sarah Galicia, Sandrine Guillard, et al. 2006. “A Genome-Wide Screen Identifies the Evolutionarily Conserved KEOPS Complex as a Telomere Regulator.” *Cell* 124 (6): 1155–68.

Ferrell, James E., Jr. 2016. “Perfect and Near-Perfect Adaptation in Cell Signaling.” *Cell Systems* 2 (2): 62–67.

Geiler-Samerotte, Kerry A., Michael F. Dion, Bogdan A. Budnik, Stephanie M. Wang, Daniel L. Hartl, and D. Allan Drummond. 2011. “Misfolded Proteins Impose a Dosage-Dependent Fitness Cost and Trigger a Cytosolic Unfolded Protein Response in Yeast.” *Proceedings of the National Academy of Sciences of the United States of America* 108 (2): 680–85.

Gidalevitz, Tali, Anat Ben-Zvi, Kim H. Ho, Heather R. Brignull, and Richard I. Morimoto. 2006. “Progressive Disruption of Cellular Protein Folding in Models of Polyglutamine Diseases.” *Science* 311 (5766): 1471–74.

Gidalevitz, Tali, Thomas Krupinski, Susana Garcia, and Richard I. Morimoto. 2009. “Destabilizing Protein Polymorphisms in the Genetic Background Direct Phenotypic Expression of Mutant SOD1 Toxicity.” *PLoS Genetics* 5 (3): e1000399.

Hahn, Ji-Sook, Daniel W. Neef, and Dennis J. Thiele. 2006. “A Stress Regulatory Network for Co-Ordinated Activation of Proteasome Expression Mediated by Yeast Heat Shock Transcription Factor.” *Molecular Microbiology* 60 (1): 240–51.

Ha, Seung-Wook, Donghong Ju, and Youming Xie. 2012. “The N-Terminal Domain of Rpn4 Serves as a Portable Ubiquitin-Independent Degron and Is Recognized by Specific 19S RP Subunits.” *Biochemical and Biophysical Research Communications* 419 (2): 226–31.

Hershko, A., H. Heller, S. Elias, and A. Ciechanover. 1983. “Components of Ubiquitin-Protein Ligase System. Resolution, Affinity Purification, and Role in Protein Breakdown.” *The Journal of Biological Chemistry* 258 (13): 8206–14.

Hershko, A., E. Leshinsky, D. Ganoth, and H. Heller. 1984. “ATP-Dependent Degradation of Ubiquitin-Protein Conjugates.” *Proceedings of the National Academy of Sciences*. https://doi.org/10.1073/pnas.81.6.1619.

Ju, Donghong, Xiaogang Wang, Haiming Xu, and Youming Xie. 2008. “Genome-Wide Analysis Identifies MYND-Domain Protein Mub1 as an Essential Factor for Rpn4 Ubiquitylation.” *Molecular and Cellular Biology* 28 (4): 1404–12.

Ju, Donghong, Haiming Xu, Xiaogang Wang, and Youming Xie. 2007. “Ubiquitin-Mediated Degradation of Rpn4 Is Controlled by a Phosphorylation-Dependent Ubiquitylation Signal.” *Biochimica et Biophysica Acta (BBA) - Molecular Cell Research*. https://doi.org/10.1016/j.bbamcr.2007.04.012.

502 Klaips, Courtney L., Gopal Gunanathan Jayaraj, and F. Ulrich Hartl. 2018. “Pathways of Cellular
503 Proteostasis in Aging and Disease.” *The Journal of Cell Biology*.
504 https://doi.org/10.1083/jcb.201709072.
505 Kraft, David Christian, Custer C. Deocaris, Renu Wadhwa, and Suresh I. S. Rattan. 2006.
506 “Preincubation with the Proteasome Inhibitor MG-132 Enhances Proteasome Activity via
507 the Nrf2 Transcription Factor in Aging Human Skin Fibroblasts.” *Annals of the New York*
508 *Academy of Sciences* 1067 (May): 420–24.
509 Labbadia, Johnathan, and Richard I. Morimoto. 2015a. “The Biology of Proteostasis in Aging
510 and Disease.” *Annual Review of Biochemistry*. https://doi.org/10.1146/annurev-biochem-
511 060614-033955.
512 Lecker, Stewart H., Alfred L. Goldberg, and William E. Mitch. 2006. “Protein Degradation by the
513 Ubiquitin–Proteasome Pathway in Normal and Disease States.” *Journal of the American*
514 *Society of Nephrology*. https://doi.org/10.1681/asn.2006010083.
515 Lundgren, J., P. Masson, C. A. Realini, and P. Young. 2003. “Use of RNA Interference and
516 Complementation To Study the Function of the Drosophila and Human 26S Proteasome
517 Subunit S13.” *Molecular and Cellular Biology*. https://doi.org/10.1128/mcb.23.15.5320-
518 5330.2003.
519 Ma, Menggen, and Z. Lewis Liu. 2010. “Comparative Transcriptome Profiling Analyses during
520 the Lag Phase Uncover YAP1, PDR1, PDR3, RPN4, and HSF1 as Key Regulatory Genes
521 in Genomic Adaptation to the Lignocellulose Derived Inhibitor HMF for Saccharomyces
522 Cerevisiae.” *BMC Genomics* 11 (November): 660.
523 Mannhaupt, G., R. Schnall, V. Karpov, I. Vetter, and H. Feldmann. 1999. “Rpn4p Acts as a
524 Transcription Factor by Binding to PACE, a Nonamer Box Found Upstream of 26S
525 Proteasomal and Other Genes in Yeast.” *FEBS Letters* 450 (1-2): 27–34.
526 Maurer, Matthew J., Eric D. Spear, Allen T. Yu, Evan J. Lee, Saba Shahzad, and Susan
527 Michaelis. 2016. “Degradation Signals for Ubiquitin-Proteasome Dependent Cytosolic
528 Protein Quality Control (CytoQC) in Yeast.” *G3* 6 (7): 1853–66.
529 Meiners, Silke, Dirk Heyken, Andrea Weller, Antje Ludwig, Karl Stangl, Peter-M Kloetzel, and
530 Elke Krüger. 2003. “Inhibition of Proteasome Activity Induces Concerted Expression of
531 Proteasome Genes and de Novo Formation of Mammalian Proteasomes.” *The Journal of*
532 *Biological Chemistry* 278 (24): 21517–25.
533 Moye-Rowley, W. Scott. “Transcriptional Control of Multidrug Resistance in the Yeast
534 Saccharomyces.” *Progress in Nucleic Acid Research and Molecular Biology*.
535 https://doi.org/10.1016/s0079-6603(03)01008-0.
536 Radhakrishnan, Senthil K., Candy S. Lee, Patrick Young, Anne Beskow, Jefferson Y. Chan, and
537 Raymond J. Deshaies. 2010. “Transcription Factor Nrf1 Mediates the Proteasome
538 Recovery Pathway after Proteasome Inhibition in Mammalian Cells.” *Molecular Cell* 38 (1):
539 17–28.
540 Ruggiano, Annamaria, Ombretta Foresti, and Pedro Carvalho. 2014. “Quality Control: ER-
541 Associated Degradation: Protein Quality Control and beyond.” *The Journal of Cell Biology*
542 204 (6): 869–79.
543 Sato, Youichi, Kozue Sakamoto, Masako Sei, Ashraf A. Ewis, and Yutaka Nakahori. 2009.
544 “Proteasome Subunits Are Regulated and Expressed in Comparable Concentrations as a
545 Functional Cluster.” *Biochemical and Biophysical Research Communications* 378 (4): 795–
546 98.
547 Satyal, S. H., E. Schmidt, K. Kitagawa, N. Sondheimer, S. Lindquist, J. M. Kramer, and R. I.
548 Morimoto. 2000. “Polyglutamine Aggregates Alter Protein Folding Homeostasis in
549 Caenorhabditis Elegans.” *Proceedings of the National Academy of Sciences of the United*
550 *States of America* 97 (11): 5750–55.
551 Schmidt, Rolf M., Julia P. Schessner, Georg Hh Borner, and Sebastian Schuck. 2019. “The
552 Proteasome Biogenesis Regulator Rpn4 Cooperates with the Unfolded Protein Response

553 to Promote ER Stress Resistance." *eLife* 8 (March). https://doi.org/10.7554/eLife.43244.
554 Shirozu, Ryohei, Hideki Yashiroda, and Shigeo Murata. 2015. "Identification of Minimum Rpn4-
555 Responsive Elements in Genes Related to Proteasome Functions." *FEBS Letters* 589 (8):
556 933–40.
557 Sorger, P. K. 1990. "Yeast Heat Shock Factor Contains Separable Transient and Sustained
558 Response Transcriptional Activators." *Cell* 62 (4): 793–805.
559 Sweeney, Patrick, Hyunsun Park, Marc Baumann, John Dunlop, Judith Frydman, Ron Kopito,
560 Alexander McCampbell, et al. 2017. "Protein Misfolding in Neurodegenerative Diseases:
561 Implications and Strategies." *Translational Neurodegeneration* 6 (March): 6.
562 Szymczak, Andrea L., and Dario A. A. Vignali. 2005. "Development of 2A Peptide-Based
563 Strategies in the Design of Multicistronic Vectors." *Expert Opinion on Biological Therapy* 5
564 (5): 627–38.
565 Temple, Mark D., Gabriel G. Perrone, and Ian W. Dawes. 2005. "Complex Cellular Responses
566 to Reactive Oxygen Species." *Trends in Cell Biology*.
567 https://doi.org/10.1016/j.tcb.2005.04.003.
568 Tye, Blake W., Nicoletta Commins, Lillia V. Ryazanova, Martin Wühr, Michael Springer, David
569 Pincus, and L. Stirling Churchman. 2019. "Proteotoxicity from Aberrant Ribosome
570 Biogenesis Compromises Cell Fitness." *eLife* 8 (March).
571 https://doi.org/10.7554/eLife.43002.
572 Voges, D., P. Zwickl, and W. Baumeister. 1999. "The 26S Proteasome: A Molecular Machine
573 Designed for Controlled Proteolysis." *Annual Review of Biochemistry* 68: 1015–68.
574 Wallace, Edward W. J., Jamie L. Kear-Scott, Evgeny V. Pilipenko, Michael H. Schwartz, Pawel
575 R. Laskowski, Alexandra E. Rojek, Christopher D. Katanski, et al. 2015. "Reversible,
576 Specific, Active Aggregates of Endogenous Proteins Assemble upon Heat Stress." *Cell* 162
577 (6): 1286–98.
578 Wang, Li, Xicheng Mao, Donghong Ju, and Youming Xie. 2004. "Rpn4 Is a Physiological
579 Substrate of the Ubr2 Ubiquitin Ligase." *The Journal of Biological Chemistry* 279 (53):
580 55218–23.
581 Wang, Xiaogang, Haiming Xu, Seung-Wook Ha, Donghong Ju, and Youming Xie. 2010.
582 "Proteasomal Degradation of Rpn4 in Saccharomyces Cerevisiae Is Critical for Cell Viability
583 under Stressed Conditions." *Genetics* 184 (2): 335–42.
584 Weids, Alan J., and Chris M. Grant. 2014. "The Yeast Peroxiredoxin Tsa1 Protects against
585 Protein-Aggregate-Induced Oxidative Stress." *Journal of Cell Science* 127 (Pt 6): 1327–35.
586 Xie, Y., and A. Varshavsky. 2001. "RPN4 Is a Ligand, Substrate, and Transcriptional Regulator
587 of the 26S Proteasome: A Negative Feedback Circuit." *Proceedings of the National*
588 *Academy of Sciences of the United States of America* 98 (6): 3056–61.
589 Xu, Haiming, Donghong Ju, Tiffany Jarois, and Youming Xie. 2008. "Diminished Feedback
590 Regulation of Proteasome Expression and Resistance to Proteasome Inhibitors in Breast
591 Cancer Cells." *Breast Cancer Research and Treatment* 107 (2): 267–74.
592 Yamamoto, Noritaka, Yuka Maeda, Aya Ikeda, and Hiroshi Sakurai. 2008. "Regulation of
593 Thermotolerance by Stress-Induced Transcription Factors in Saccharomyces Cerevisiae."
594 *Eukaryotic Cell* 7 (5): 783–90.
595 Zheng, Xu, Joanna Krakowiak, Nikit Patel, Ali Beyzavi, Jideofor Ezike, Ahmad S. Khalil, and
596 David Pincus. 2016. "Dynamic Control of Hsf1 during Heat Shock by a Chaperone Switch
597 and Phosphorylation." *eLife* 5 (November). https://doi.org/10.7554/eLife.18638.

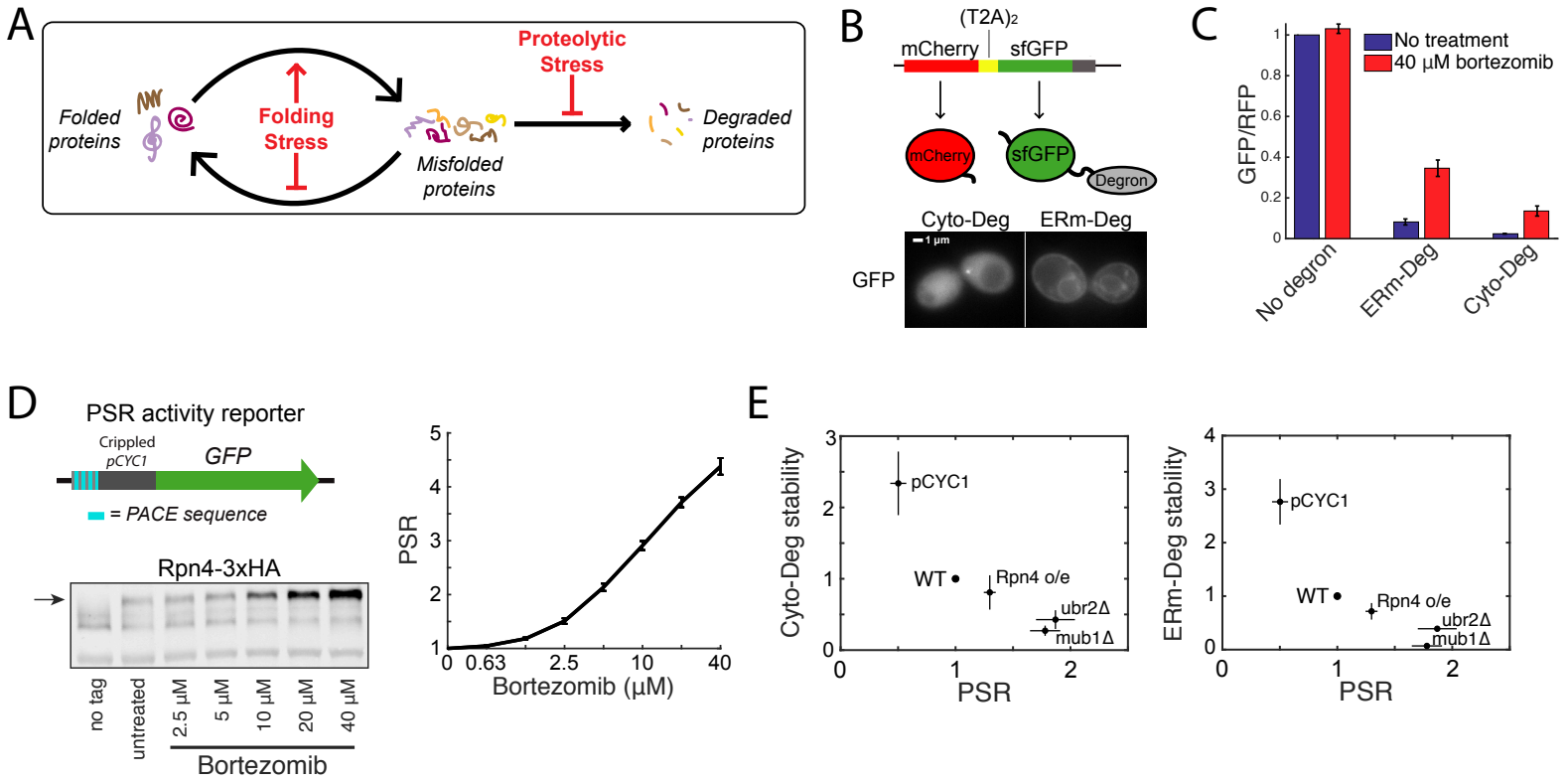

Figure 1: Clearance of defective proteins scales with the PSR. A: Diagram of protein folding and degradation, and the effect of folding and proteasomal stress. **B:** (Top) Schematic of T2A system for controlled expression of degron reporters. (Bottom) GFP localization of Cyto-Deg and ERm-Deg in normal conditions. **C:** Mean RFP-normalized GFP fluorescence of Cyto-Deg, ERm-Deg, and a no degron control with either 0 µM (blue bars) or 40 µM (red bars) bortezomib. **D:** (Top left) Schematic of PSR activity reporter. (Bottom left) Immunoblot of HA-tagged endogenous Rpn4 under a serial titration of bortezomib. Arrow indicates the position of Rpn4-3xHA. (Right) Mean forward scatter normalized GFP of PSR activity reporter under a serial titration of bortezomib. Units are fold change from no treatment. **E:** Plots of fold degron stability (Left panel: Cyto-Deg; Right panel: ERm-Deg) versus fold PSR upon modifying Rpn4 levels through deletion of *UBR2* or *MUB1*, replacement of the endogenous *RPN4* promoter with *pCYC1*, or expression of a second copy of *RPN4* from a plasmid. Error bars denote standard error for n≥3 biological replicates.

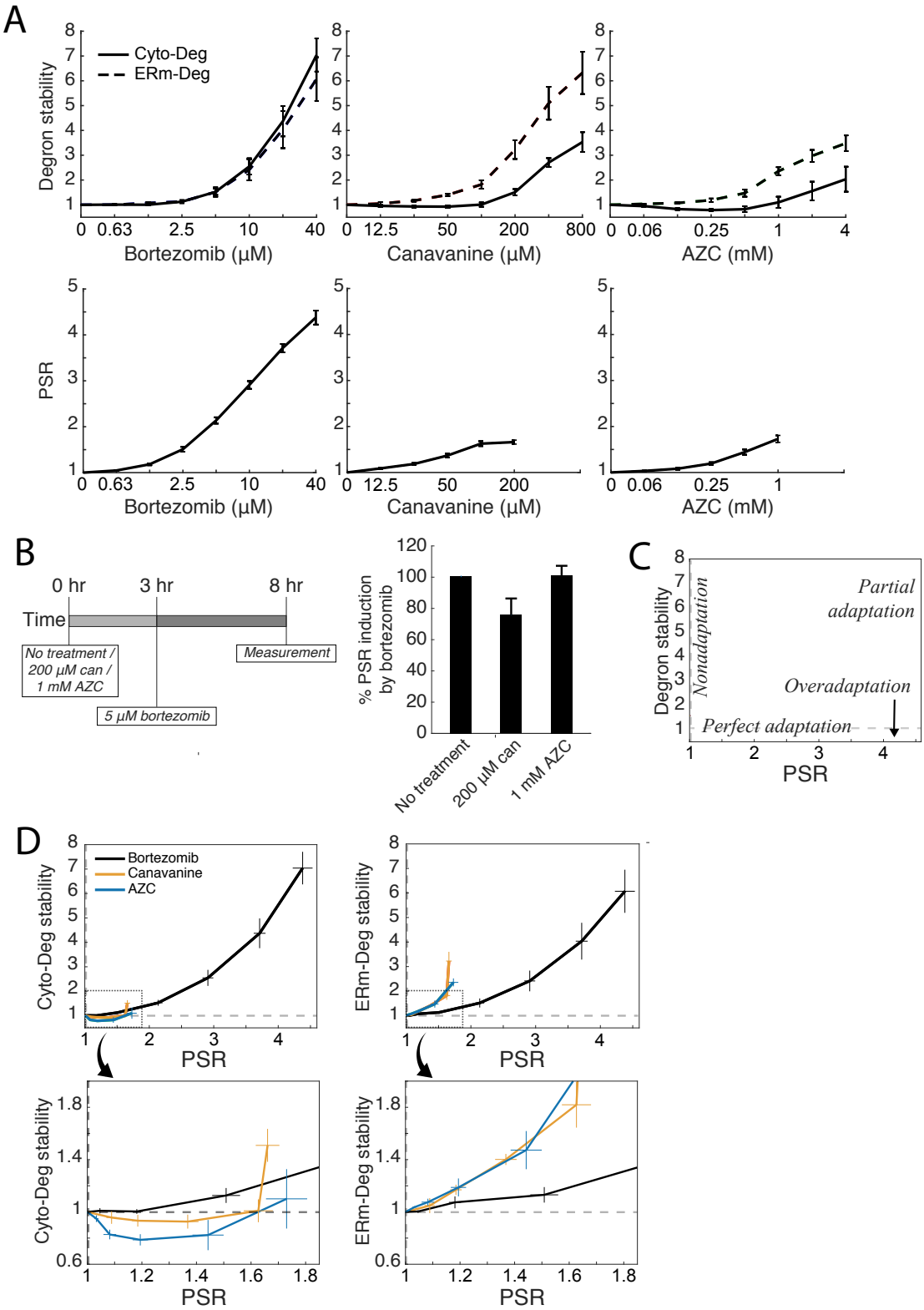

Figure 2: Proteotoxic stressors elicit multiple adaptive regimes. A: Measurements of fold degron stability (top row, solid: Cyto-Deg, dotted: ERm-Deg) and fold PSR activity (bottom row) in titrations of bortezomib, canavanine, or AZC. **B:** Measurement of PSR activity (right) after treatment with 5 μM bortezomib and either 200 μM canavanine, 1 mM AZC, or no additional treatment, at the noted time points (left). **C:** Schematic of adaptive regimes as a function of degron stability and PSR activity. **D:** Plots of fold degron stability (left: Cyto-Deg, right: ERm-Deg) versus fold PSR activity for the titrations in (A) to reveal the adaptive regime for each stressor. The boxed regions in the upper plots are enlarged in the lower plots. Error bars denote standard error for n≥3 biological replicates.

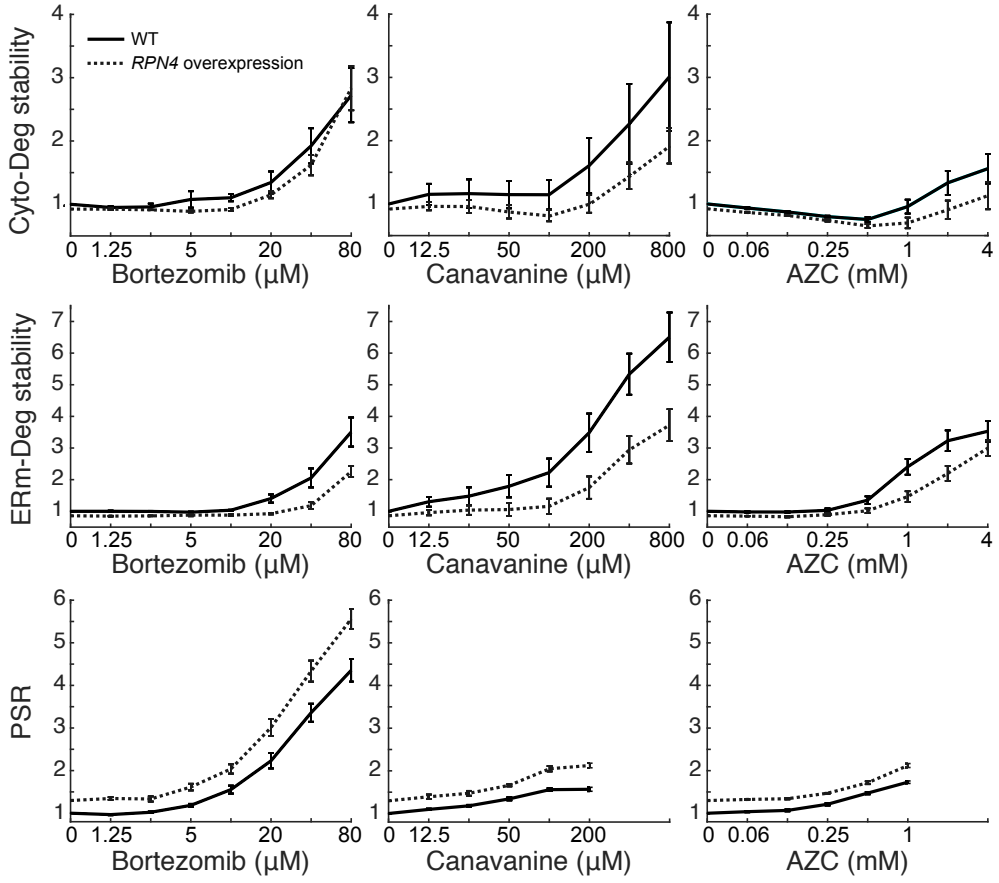

Figure 3: Boosting the PSR improves UPS performance under stress. Measurements of fold degron stability (top: Cyto-Deg, middle: ERm-Deg) and fold PSR activity (bottom) in titrations of bortezomib, canavanine, or AZC for cells expressing an empty vector (black) or a second copy of *RPN4* (dotted). Error bars denote standard error for n≥3 biological replicates.

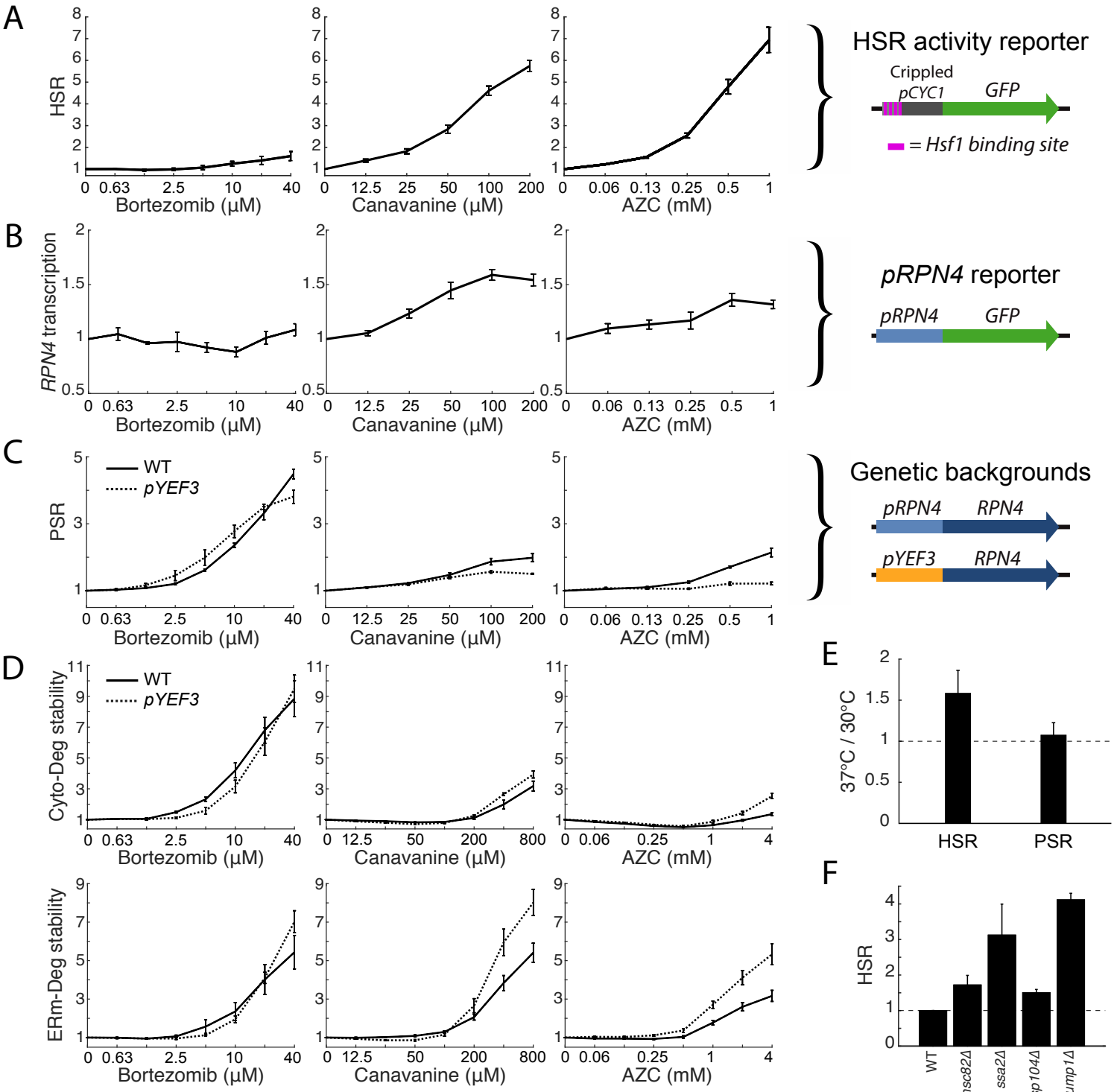

Figure 4: Folding stressors activate the PSR via transcription of RPN4 and do not increase UPS substrate load. A: Schematic of a HSR reporter (right) and its fold GFP induction in titrations of bortezomib, canavanine, and AZC (left). **B:** Schematic of a pRPN4 reporter (right) and its fold GFP induction in titrations of bortezomib, canavanine, and AZC (left). **C:** Schematic of the RPN4 locus in wildtype or a pYEF3:RPN4 background (right), and measurements of fold PSR activity in stressor titrations for both strains (left). **D:** Measurements of Cyto-Deg (top) and ERm-Deg (bottom) fold stability for titrations of bortezomib, canavanine, or AZC in either a wildtype (solid) or pYEF3:RPN4 (dotted) background. Titrations of both strains are normalized to the no-treatment values of each reporter. **E:** Mean fold activity of the HSR or PSR at 37°C relative to 30°C in wildtype cells. **F:** Mean fold activity of the HSR (left) or PSR (right) relative to wildtype upon deletion of HSC82, SSA2, HSP104, or UMP1. Error bars denote standard error for n≥3 biological replicates.

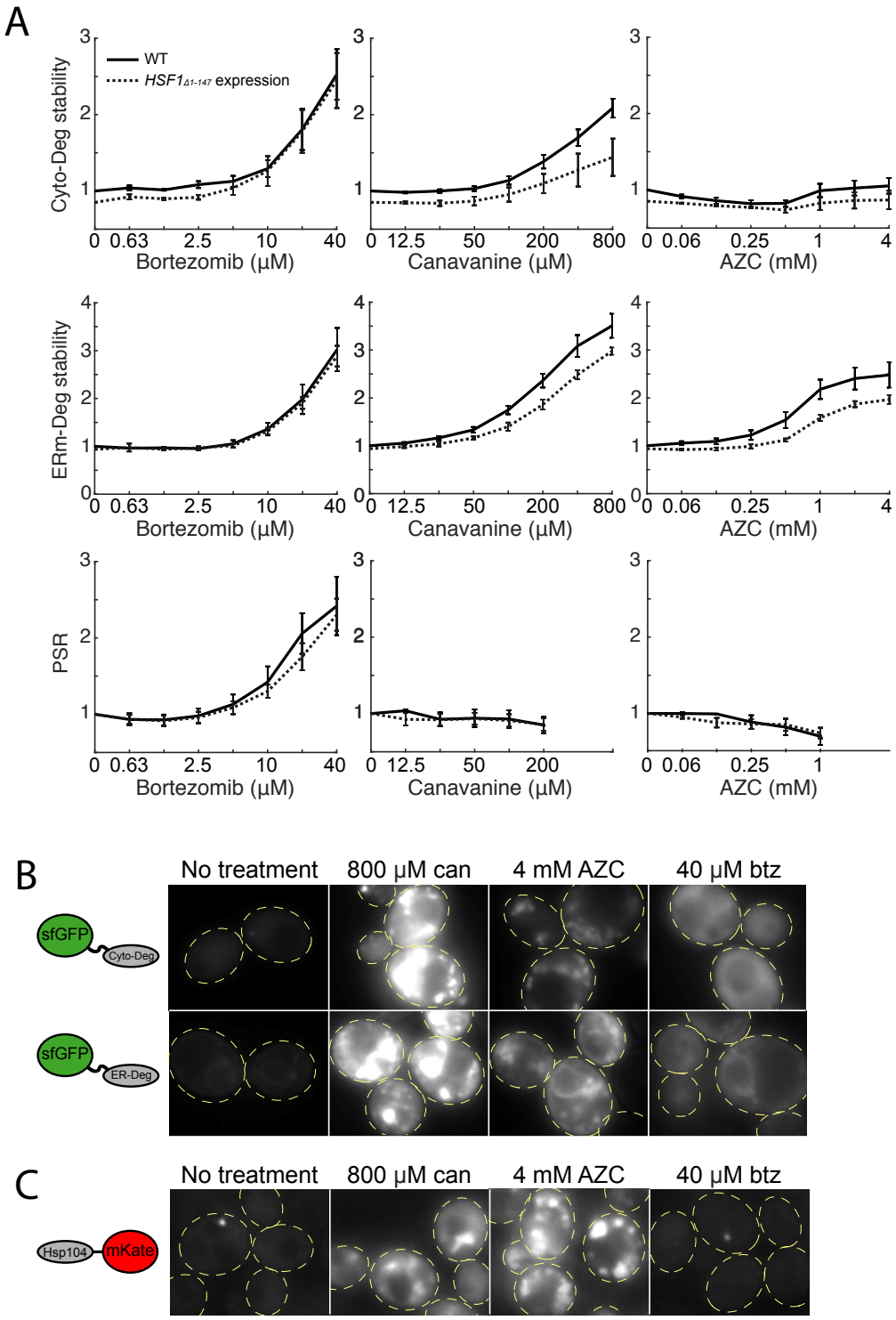

Figure 5: Folding stressors cause aggregation and result in failure to target aggregation-prone substrates to the proteasome. A: Measurements of fold degron stability (top: Cyto-Deg, middle: ERm-Deg) and fold PSR activity (bottom) in titrations of bortezomib, canavanine, or AZC for cells expressing an empty vector (solid) or a copy of HSF1Δ 1-147 (dotted). **B-C:** Fluorescent localization of ERm-Deg (GFP), Cyto-Deg (GFP), or Hsp104-mKate2 (RFP) in cells treated with 800 μM canavanine, 4 mM AZC, 40 μM bortezomib, or no treatment for 5 hours. Cells are outlined in yellow dashed lines.

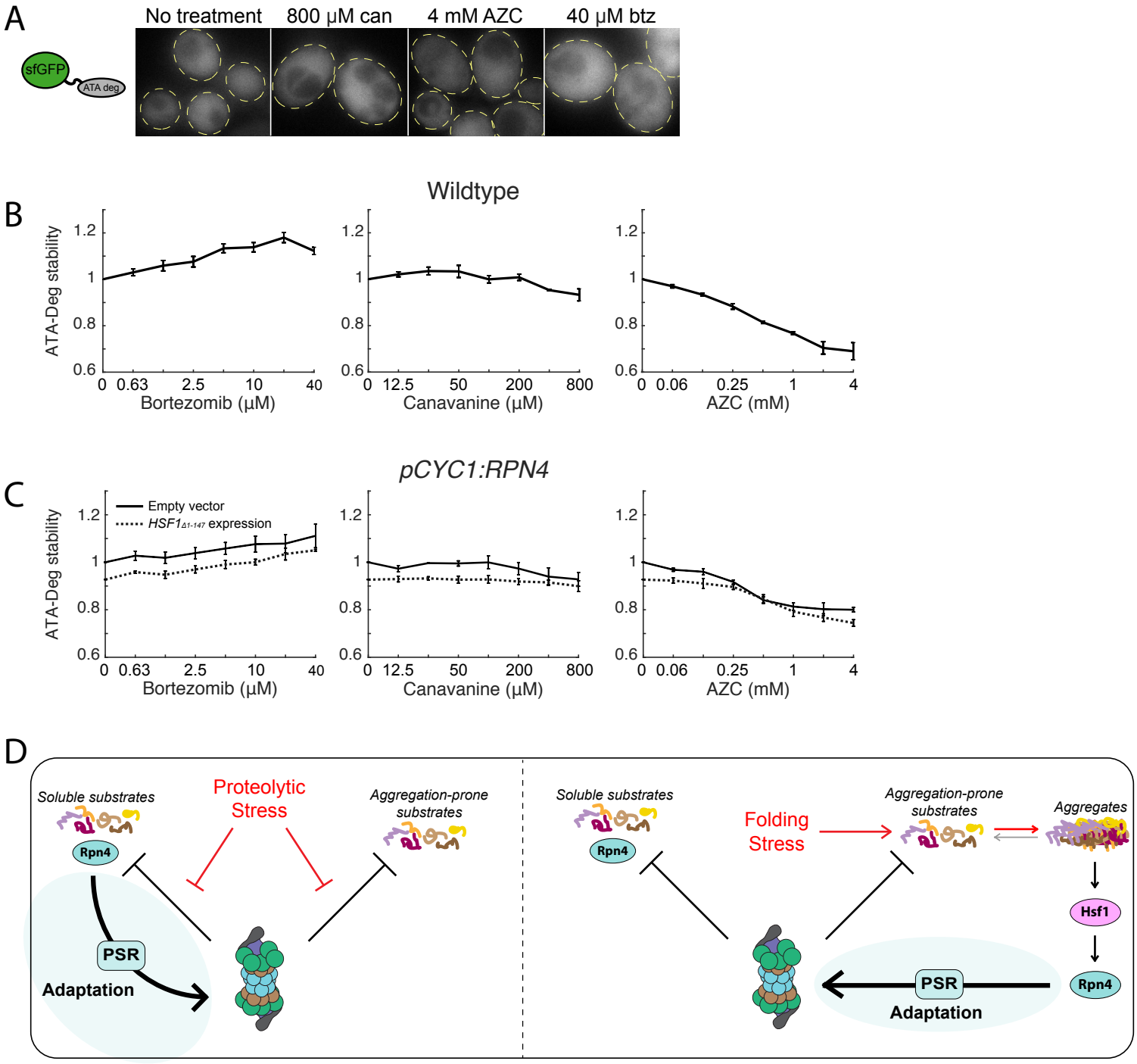

Figure 6: Folding stressors do not impair degradation of soluble UPS substrates. A: Fluorescent localization of ATA-Deg (GFP) in cells treated with 800 μM canavanine, 4 mM AZC, 40 μM bortezomib, or no treatment for 5 hours. Cells are outlined in yellow dashed lines. **B:** Measurements of fold ATA-Deg stability in titrations of bortezomib, canavanine, or AZC. **C:** Fold ATA-Deg stability in drug titrations in cells expressing an empty vector (solid) or a copy of HSF1Δ 1-147 (dotted). Error bars throughout denote standard error for n≥3 biological replicates. D: Model for UPS adaptation by the PSR to proteolytic and folding stressors. (Left) Proteolytic stressors increases the stability of all proteasome substrates. This includes Rpn4, whose accumulation leads to PSR activation. (Right) Folding stressors causes some proteasome substrates to sequester into aggregates. Aggregation triggers the HSR, activates transcription of RPN4, and causes PSR activation.